sciendo

Civil and Environmental Engineering
Vol. 20, Issue 1, 440-460, DOI: 10.2478/cee-2024-0034

EMPIRICAL MODELING OF HIGH-PERFORMANCE SELF-COMPACTING CONCRETE WITH INDUCTION-FURNACE SLAG

Oluwaseun MARK[1,*], Anthony EDE[1], Chinwuba ARUM[2], Kayode JOLAYEMI[1]

[1] Department of Civil Engineering, College of Engineering, Covenant University, km 10, Idiroko Road, Sango, Ota, Ogun State, PMB 1023, Nigeria.
[2] Department of Civil Engineering, School of Engineering and Engineering Technology, Federal University of Technology, Akure, Ondo State, PMB 704, Nigeria.
[*] corresponding author: oluwaseun.mark@covenantuniversity.edu.ng

Abstract

This study led to the creation of empirical models of the properties of high-performance self-compacting concrete (HPSCC) with induction-furnace slag (IFS) added as an extra cementitious ingredient. The ingredients were Portland cement, IFS ranging from 0 to 50% by cement weight, granite, river sand, water, and superplasticizer. Using a slump flow test, the filling-ability property of the newly produced HPSCC was investigated. Similarly, a compressive strength test was used to determine the hardened HPSCC's compressive strength. Using already established scientific ideas, the empirical model of the filling-ability characteristic of the fresh HPSCC was generated, on the basis of the slump flow and the volume of the paste of the fresh concrete. Likewise, the empirical model of the compressive strength of the hardened HPSCC was generated, based on the combination of the parameters of the strength developed over time, with the strength developed, due to the addition of the IFS. Based on these, the empirical model of the filling-ability property of the fresh HPSCC was $\frac{\rho}{s_{f^2}} = 0.002(1 - V_P)^{-11.34}$, while that of the compressive strength of the hardened HPSCC was $f_c\,(t) = \frac{t}{4.52+0.78t}$ (-0.0109$(P_{ifs})^2$ + 0.2632P_{ifs} + 52.446). The empirical models were then validated using test data from this work. Strong links between the measured and the predicted values were identified by the empirical correlations, where the coefficient of determination (R^2) value for the filling ability property, gave above 94% and the R^2 value for the compressive strength, gave above 86%. The estimated slump flow and the compressive strength were approximately equal to the experimental values. The outcomes demonstrated that IFS may be utilized to produce an eco-friendly and environmentally sustainable HPSCC. The models can be adopted in designing HPSCC containing IFS as a supplementary cementitious material (SCM) and in predicting its filling-ability and compressive strength, which will benefit the construction industry.

Keywords:

Concrete;
Filling-ability;
High performance self-compacting concrete;
Induction furnace slag;
Modeling;
Strength.

1 Introduction

Concrete remains the most predominant construction material used in the construction industry. It is more often used currently than ever before [1]. Report has it that about 1.5 billion metric tonnes of concrete are consumed annually [2]. Due to more constructions, the consumption of concrete is expected to be on a high rise, as each year goes by. However, it is of great concern that the production of concrete will pose negative effects on the environment. For instance, a typical batch of concrete has a bulk composition of 80% aggregate, 12% cement, and 8% water for mixing [3]. Consequently, 1.5 billion tonnes of cement, 9 billion tonnes of aggregates, and 1 billion tonnes of water are needed each year for the manufacturing of concrete. As a result, the annual production of concrete causes issues for the environment such as significant emissions of greenhouse gases (GHG) into the atmosphere, depletion of natural resources, and increased energy demand. The cement industry previously exclusively produced regular Portland cement. To reduce the environmental impact of cement

manufacture, some of the clinker has been replaced with additional cementitious materials for many years. The use of SCMs in concrete production has several benefits, including an alternate application for non-recyclable solid wastes from dumps and landfills, overcoming cement manufacture's negative consequences, reduced energy consumption, and lower greenhouse gas emissions [4]. The need to produce more concrete in the construction industry and the effort to protect the environment, make the use of non-recyclable solid waste and industrial waste products as concrete constituents more important because it provides effective management of such wastes, more natural resources and energy are conserved, also, it provides a more durable as well as a high-performance concrete [5].

Self-compacting concrete and high-performance concrete (concrete with high strength and durability) are combined to create high performance self-compacting concrete (HPSCC) (concrete with high flowing ability and adequate resistance to segregation under its own weight, with no form of compaction). Therefore, HPSCC can be defined as the concrete with high strength, excellent durability, good flowability and excellent resistance to aggregate segregation [6]. HPSCC is typically different from the ordinary concrete in the sense that it contains additional constituents such as superplasticizers as well as supplementary cementitious materials which are not present in the ordinary concrete. Likewise, the ratio of the constituents is not the same as with the ordinary concrete. HPSCC contains more binders, lesser water/binder proportion, more fines, lesser coarse aggregates than the ordinary concrete [7].

Assessment of complex methods needs unique evidence of the required standard characteristics which shows result of the method as well as parameters associated with the features. When the analyses of the parameters are done, characteristics of the correlations among the parameters are assessed. Experimental design carries more value than mere tabulation. When a test is well-designed and carried out, assessment of the result needs to reference the complexity of the method [8].

The slump flow is a key fresh property that expresses the filing ability of HPSCC. Murata [9] generated an empirical model between the yield stress and the slump flow of an SCC. The empirical model considered the friction resistance between rubber sheets and the concrete. Having a slump flow range of values between 500 mm and 850 mm and a yield stress range of values between 0 Pa and 1000 Pa, he concluded that the model is valid for concrete. As a result, HPSCC can benefit from the concept. Additionally, a study was conducted by developing an empirical model connecting a freshly mixed concrete's yield stress, plastic viscosity, slump flow, and slump flow time. [10]. They found out that the model can be used for any type of concrete in its fresh state, which also includes HPSCC. They likewise concluded that the varying slump cone shape factor, determines the accuracy of the model. Another study [11] simply created a model relationship between the yield stress, plastic viscosity, slump flow, and slump flow duration to eliminate the influence of the shape factor. The empirical model can be used to calculate the HPSCC's plastic viscosity and yield stress.

A model was generated, considering the silica fume's impact on the compressive strength concrete with high performance, comprising of sulphate-resisting cement as well as ordinary Portland cement. It was found out that the model was valid for up to 28 days curing age of the concrete [12]. Another empirical model was also done, investigating the impact of a selected supplementary cementitious material on the crushing strength of a high-performance concrete (HPC). It was also discovered that the model was valid for crushing strength of the HPC, up to 28 days of curing [13]. An empirical model was formulated for the compressive strength of a high-performance concrete, combining the contents of silica fume as SCM, water-binder proportion as well as the contents of the coarse aggregate as the factors in the functions. The cement type utilized was the high early strength cement. The empirical model was validated for the 28 days' compressive strength of the HPC [14]. A report on the empirical modeling of a high-performance concrete, containing blast furnace slag as an SCM suggested that the model can be applied in estimating the crushing strength of HPC at any curing age [15].

Model was generated for an HPSCC [16]. The rheology of the paste, the distance between the aggregates in the concrete as well as the sizes of the aggregates were considered in this model. Discussions were done on the aggregate segregation, the flowing-ability, the deformation as well as the stability of the concrete, from this model. Medium strength as well as normal strength models of self-compacting concrete were likewise generated in a research [17]. The factors considered were the contents of cement, supplementary cementitious material and the water reducing agent. While the responses were the compressive strength characteristics as well as the properties of the fresh SCC. It was concluded that the model will be useful in successfully predicting the constituents of the self-compacting concrete in years to come, which will help in reducing the total number of trials and thereby reducing time and cost.

The previously discussed models were found to be peculiar to self-compacting and high-performance concrete, both of which have water/binder ratio below 0.40. On the basis of the experimental study, they can therefore be applied to high performance self-compacting concrete that includes induction furnace slag as an additional cementitious ingredient.

Waste is produced when cast iron and ductile iron are produced in an induction furnace in a foundry. This waste is known as slag from an induction furnace. Slags are defined as metallic and non-metallic oxides that have been chemically mixed and may also contain gases, metallic sulphides, and trace amounts of minerals [18]. The slags from the foundry sites are disposed of by foundry workers, who consequently pollute the soil and decrease its fertility. Between 10 and 15% of these metals are present in induction furnace slag (IFS). Numerous foundries disregard these special metals. Ordinary blast furnace slag (BFS) and induction furnace slag (IFS) differ in that the former is basic in nature and the latter is acidic, due to the difference in their methods of production. IFS is produced from induction process (anaerobic condition), while BFS is produced from combustion process (aerobic condition) [19]. To obtain the powder from the slag stone, the IFS stone was pulverized, milled and sieved through 45 μm sieve [3]. Utilizing IFS as an SCM will lower HPSCC manufacturing costs, lowering the environmental stress brought on by the issue of waste disposal. IFS also reduce the amount of cement used while making concrete., thereby reducing the cost of producing concrete as well as reducing the negative environmental impact, caused from cement production. Therefore, partially replacing cement with IFS improves the characteristics and reduces the cost of producing HPSCC as well as improves the environment [4].

Little has been done up to this point to evaluate and create empirical models for the filling ability, which is a key characteristic of the fresh HPSCC and compressive strength, which is also a key property of the hardened of HPSCC, containing induction furnace slag as an alternative to cement. When IFS is introduced into the HPSCC, this work aims to empirically analyse the fresh and strength properties of the concrete. Empirical models for the fresh HPSCC's filling-ability (slump flow) as well as for the compressive strength of the hardened HPSCC were generated and validated via the experimental data from this research. In order to achieve the aim of this study, earlier mentioned, the objectives of this study were to; investigate the physical and chemical characteristics of the constituents used in making the HPSCC; determine the filling-ability property of the fresh HPSCC, via the slump flow test; determine the compressive strength of the hardened HPSCC, via the compressive strength test; generate the empirical models for the filling-ability and the compressive strength of the HPSCC, using already established scientific ideas, and finally; validate the generated models.

2 Experimental procedures

Fig. 1 shows the road map of this study.

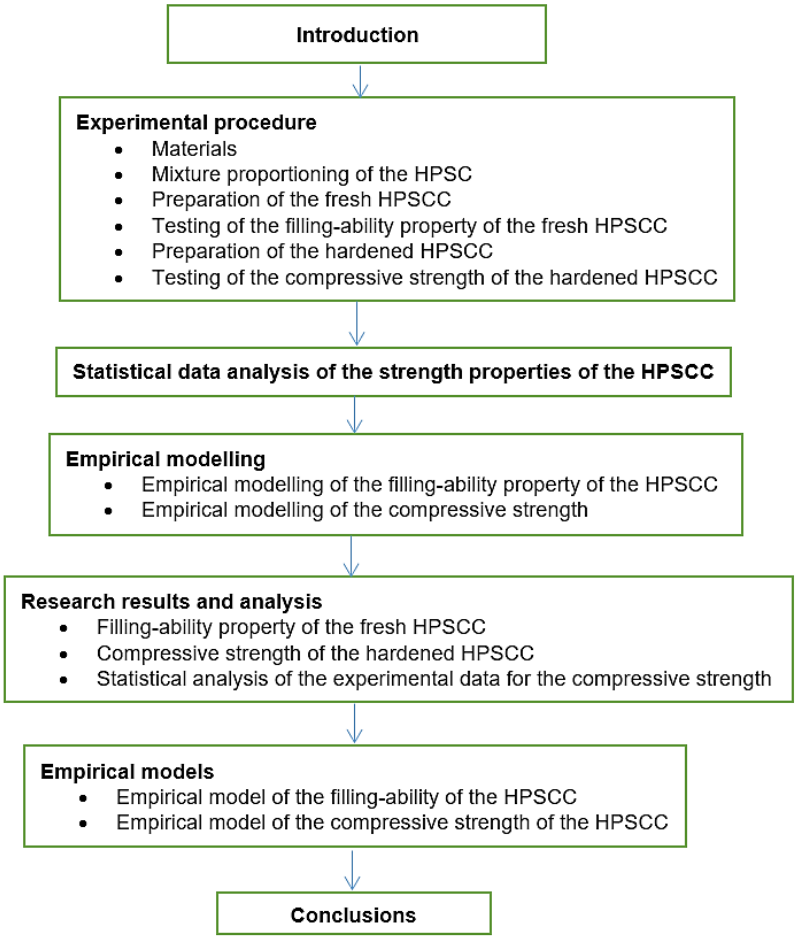

Fig. 1: Road map of the study.

2.1. Materials

In order to achieve the first objective, as pointed out in section 1, the materials selected for this study are discussed in this section. Each material chosen is a major and generally-known constituent of high performance self-compacting concrete, except for the induction furnace slag, which is the new material introduced and investigated in this study.

42.5R Portland Cement was used as the material binder in the experiment for this study. This is a type I multi-purpose cement that meets ASTM C150 standard [20]. It was obtained at a retail outlet in Ota, Ogun State, Nigeria. In Table 1 and Table 2, the cement's physical and chemical properties are listed, respectively.

The induction furnace slag (IFS) used for the experiment in this research, as shown in Fig. 2a), was locally sourced at Nigeria foundries limited, Sango, Ota, Ogun State, Nigeria. The slag was found to be readily available and abundant at the foundry dumping site. Using a steel ball rolling mill, at Highway/Transportation Laboratory of Covenant University, Ota, Ogun State, Nigeria, the big sized slags were reduced and sieved to a fineness of 43 µm, conforming to cement grading requirement. Table 1 and Table 2 list the physical and chemical features of the IFS, respectively.

Sharp sand at a natural pit in Ota, Ogun State, Nigeria, with particle fineness passing through a 4.75 mm sieve, as seen in the particle size distribution curve of Fig. 3a), served as the fine aggregate for the experiments in this study. Table 3 shows the fine aggregate's physical characteristics.

Locally accessible granite was procured from a quarry site in Abeokuta, Ogun State, Nigeria, in the form of a mixture of crushed and round aggregate. The granite had a nominal size of 12.5 mm, as seen from the particle size distribution curve in Fig. 3b). 50% of the total aggregate weight was made up of rounded aggregate. Table 3 presents the physical attributes of the coarse aggregate.

Conplast SP 430 super plasticizer, a Polycarboxylate-based high range water reduction agent (HRWRA), as seen in Fig. 2b), was employed to give the concrete the necessary ability to flow in accordance with ASTM C494/C494M [21]. It was a dark brown liquid.

For the mixing and curing of the concrete, potable water was used. The water's purity allowed it to be free of contaminants and fit for human consumption.

a) b)

Fig. 2: Materials added to the concrete: a) induction furnace slag, b) Conplast SP 430 super plasticizer.

Table 1: Physical characteristics of the binders used.

Property	42.5 R Portland cement	Induction furnace slag	Standard
Standard Consistency [%]	30	33	25 – 35 [20]
Initial Setting Time [minutes]	38	90	30 minimum [20]
Final Setting Time [minutes]	410	580	600 maximum [20]
Fineness [%]	6	8	10 maximum [20]
Specific Gravity	3.06	2.95	2.30 – 3.25 [20]

Table 2: Chemical composition of the binders used [20,22].

Oxide composition [%]	42.5 R Portland cement	Standard range of values for OPC	Induction furnace slag	Standard range of values for slag cement
Al_2O_3	4.98.	4 - 12	11.10	10 - 17
SiO_2	20.09	18 - 26	44.57	31 - 45
Fe_2O_3	1.80	1 - 6	22.97	10 - 40
Na_2O	0.21	≤ 1.0	0.44	-
CaO	64.19	58 - 66	5.52	4 - 20
K_2O	0.53	≤ 1.0	0.30	-
MnO	-	-	9.65	-
MgO	1.92	1 - 3	1.62	-
SO_3	1.80	0.5 – 2.5	0.33	-
P_2O_3	-	-	0.08	-
LOI	0.08	10.0 maximum	9.97	10 maximum

Table 3: Physical characteristics of the aggregates used.

Physical Characteristics	River Sand	Granite	Standard
Natural Moisture Content [%]	0.8.	0.09	7 maximum [23]
Bulk Density [kg/m^3]	1779	1671	1200 – 1750 [23]
Specific Gravity	2.64	2.66	2.50 – 3.00 [23]
Water Absorption [%]	0.85	0.75	4.5 maximum [23]
Void Content [%]	32.6	37.20	28 – 52 [23]

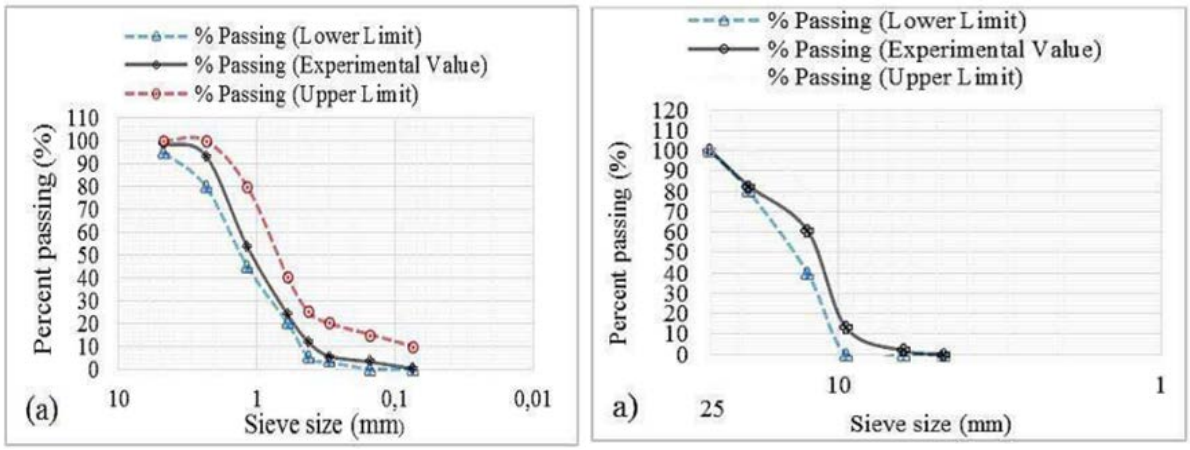

a) b)

Fig. 3. Particle size distribution (gradation) curve of: a) river sand, b) granite.

From Table 1, the fineness of the cement satisfied the requirement of the ASTM standard [20]. The specific gravity of the Portland cement was also within the limits [20]. Thus, the Portland cement was physically suitable to produce the concrete mixes for this study. According to the results of the standard consistency test, the water content satisfied the relevant standard [20]. Therefore, the setting times were tolerable for use in this study. The chemical properties of the cement used are presented in Table 2. The cement used satisfied the chemical composition stipulated by standard code [20]. It chiefly comprised of various metallic oxides. Magnesium oxide (MgO) and sulphur trioxide (SO_3) levels in the cement were below the maximum allowable levels. Magnesium oxide and sulphur trioxide in excess amounts produce cement that is unsound. Also, the resulting cement stains concrete, causes efflorescence as well as alkali aggregate reactions. Table 2 also lists the main cement constituents that were used in this study. The amounts of the chemicals in cement were within the expected range [20]. The amount of insoluble residue in the cement utilized was also minuscule. It primarily results from gypsum impurities. The cement's loss on ignition was less than the ASTM's permitted upper limit [20]. Pre-hydration and/or carbonation caused by cement's exposure to the atmosphere during lengthy storage are indicated by a larger loss on ignition.

The IFS had a specific gravity within the normal range of the majority of IFS sources [24], as seen in Table 1. The IFS was more finely ground than the cement that was used [22]. The strength of concrete is influenced by the binder's or cementing material's fineness. The strength of concrete increases with increasing binder fineness. Therefore, the higher fineness of IFS suggests that it would increase the compressive strength of concrete, in relation to achieving the third objective of this study. In contrast, the inclusion of IFS would result in less concrete being able to flow. This is due to the fact that increased fineness increases water demand while decreasing the amount of unused water in concrete. The ASTM standard [25] specified that for a material to be regarded as pozzolan, the summation of aluminium oxide, silicon oxide and iron oxide must give at least 70% of the total oxide composition. From the result obtained in Table 2, $Al_2O_3 + SiO_2 + Fe_2O_3$ for IFS gave 78.63%. This complied with ASTM standards. Since silicon dioxide (SiO_2), a siliceous substance, makes up the majority of IFS, it can be referred to as a siliceous substance. When moisture is present, calcium hydroxide $Ca(OH)_2$ from Portland cement reacts with siliceous substances to form hydraulic cementitious materials known as calcium silicate hydrate (CSH) gel. The major oxide composition of the IFS that adds to the pozzolanicity as well as the secondary hydration of the concrete is the silicon dioxide. Magnesium and sulphur were likewise found in minute quantities in IFS. For IFS, there are no ASTM chemical specifications. IFS can, however, meet the chemical specifications for blast furnace slag. For blast furnace slag, 10% loss on ignition is the maximum permitted value [22]. The loss on ignition for IFS was lower than 10%. Therefore, even with the potentially reactive materials, the IFS was suitable for use in concrete.

The physical characteristics results shown in Table 3 revealed that the river sand can be utilized in making the HPSCC, as it satisfied the standard requirements. The result of the water absorption was within the range specified by ASTM standard [23], for water absorption of fine aggregates. Being in the lower limit, it is advantageous in the strength and durability of the concrete. Also, the natural moisture content of river sand was below the maximum allowable percentage [26]. The result of the bulk density of the river sand was higher than the bulk density of the granite. Fine aggregate bulk densities are

usually greater than the coarse aggregate bulk densities because of the minimum voids present in fine aggregates [27]. The river sand had a void content lesser than the granite. According to Kosmatka et al. [27], the standard range of the void content of aggregates, suitable for use in concrete making is as shown in Table 3. Since the void content of the river sand was within this range, it made the workability (in terms of the filling ability) property of the HPSCC to still be within the acceptable range of values). The river sand had a specific gravity lower than that of the granite. As a result, the granite was slightly heavier than the river sand. Concrete segregation increases when there is a significant disparity between the relative densities of fine and coarse particles. Fig. 3a) displays the river sand gradation gotten using the sieve analysis. The concrete sand was regarded as being of good quality. Additionally, the grading of various grades of concrete sand was done according to ASTM [28] guidelines. The sieve analysis yielded the nominal maximum size of river sand. The nominal maximum size of the river sand was 4.75. The nominal size of the river sand was that acceptable for use, in making an HPSCC. Therefore, the nominal size did not impair the workability (in terms of the filling-ability) and the performance of the concrete. The total surface area of the aggregates, which determines the water consumption, and the compressive strength of the concrete mixture are both impacted by the gradation of the fine aggregate. As a result, it affects the concrete mixture design. Additionally, the fine aggregate gradation influences the physical packing of the constituent materials in concrete as well as the flow characteristics of mortar [29]. As a result, the HPSCC's characteristics may be impacted by sand gradation.

The granite was suitable for use as coarse aggregate in the production of HPSCC, according to the test results for its physical qualities, which are shown in Table 3. The outcomes fell within the parameters that standards allow for. The granite had a specific gravity within the standard range [23]. The granite absorbed water within the typical range for coarse aggregate water absorption [23]. As a result, the value is favourable in terms of concrete strength and durability because it was at the lower end of the range. For a granite that is highly porous and has a high-water absorption value, the strength and durability of the concrete may be negatively impacted. The granite's bulk density was also within the typical range [23]. The pores and voids that exist in aggregates are included. Based on the bulk density, the granite's void content was calculated. As a result, the percentage of voids between the compacted aggregates is represented by the void content. The typical range of void content for coarse aggregates is as shown in Table 3 [27]. Since the void content of the granite was within the acceptable range, it made the workability (in terms of the filling ability) property of the HPSCC to still be within the acceptable range of values). The utilized concrete stone was air-dried. The granite's surface did not contain any free water. Because of this, the granite had a very low natural moisture content. The granite used was well-graded, as evidenced by the gradation of the granite as determined by the sieve analysis and shown in Fig. 3b). Additionally, the grading of the granite's various sizes fell within the higher and lower bounds established by ASTM code [28]. The majority of the concrete stone fell between the 19 mm and 9.5 mm coarser sieve sizes. The nominal size of the granite was that acceptable for use, in making an HPSCC. Therefore, the nominal size did not impair the workability (in terms of the filling-ability) and the performance of the concrete. The workability or flowability of concrete is influenced by the gradation of the granite or coarse particles. This is so that concrete's necessary water and cement content can be affected. Since the gradation has an impact on the packing conditions of the aggregates, it also affects the segregation resistance of concrete [30]. Therefore, HPSCC's capacity to flow and resistance to segregation may be negatively impacted by coarse particles that are not properly graded. The gradation also shows the coarse particles' maximum size. During sieve analysis, it was discovered that the granite had a nominal maximum size of 19 mm. The amount of water required for a particular flowing ability depends on the coarse aggregate's maximum size. The needed water content lowers as the maximum size increases. Additionally, the cement content is decreased by raising the maximum size of coarse aggregate [27]. As a result, the maximum size of coarse aggregate has a big impact on how concrete mixtures are designed.

2.2 Mixture proportioning of the HPSCC

The HPSCC's control mix was designed to a target strength of 40 MPa, at 28 days. This is in line with the works of Farhad et [6] and Ma [7], that the minimum compressive strength of an HPSCC at 28 days must be 40 MPa. This relates to the practical application of HPSCC in construction in the sense that, if the HPSCC produced is less than 40 MPa, it cannot be used as a high-performance self-compacting concrete in construction.

As a supplementary cementitious material, various percentage replacement levels of induction furnace slag (IFS) were used to create various HPSCC mixes. On the basis of preliminary testing and also based on the findings of previous researchers, who investigated on the use of IFS in making conventional concrete [18, 19], 0%, 10%, 20%, 30%, 40% and 50% percentage replacement levels were chosen. In practical sense, it is easier to partially substitute cement at those replacement levels during the batching of the concrete constituents than at lower percentage replacement levels.

Six (6) different kinds of HPSCC combinations were created in total. Table 4 lists the names and descriptions of the concrete mixtures. By weight of the binder component, the super plasticizer percentage was 0.02, the water/binder ratio was 0.36, and the concrete mix ratio was 1:1.02:0.95. On the basis of the IFS content, the concrete mixtures were created. For instance, a high-performance self-compacting concrete made with 100% cement and 0% IFS content was given the name "HPSCC0,100".

Table 4: Designed HPSCC mixes.

S/N	Concrete Type	Cement [kg/m^3]	IFS [kg/m^3]	River Sand [kg/m^3]	Granite [kg/m^3]	Water [kg/m^3]	Super plasticizer [kg/m^3]
1	HPSCC0,100.	733.0	0	747.66	696.35	263.88	14.66
2	HPSCC10,90	659.7	73.3	747.66	696.35	263.88	14.66
3	HPSCC20,80	586.4	146.6	747.66	696.35	263.88	14.66
4	HPSCC30,70	513.1	219.9	747.66	696.35	263.88	14.66
5	HPSCC40,60	439.8	293.2	747.66	696.35	263.88	14.66
6	HPSCC50,50	366.5	366.5	747.66	696.35	263.88	14.66

2.3 Preparation of the fresh HPSCC

The fresh HPSCC mixes were made in accordance with the prescribed procedures [31]. The binders were first mixed thoroughly, to ensure a uniform blend, the fine aggregate was added and further mixing was done to a uniform blend, the coarse aggregate was later added and were all mixed thoroughly, to a uniform blend too. The superplasticizer was added to the water and mixed thoroughly too. The water containing the superplasticizer was poured into the already mixed constituents and final mixing was done, until the fresh concrete looked homogeneous in appearance and a good consistency was achieved. Prior to batching, the batch volume of the concrete mixtures was estimated. To account for losses at the time the concrete was mixed and tested, the amount of the new HPSCC batch was raised by 15%. The modifications made to the mix proportions were used to calculate the amounts of the principal constituent materials for each batch of the concrete, while the constituents were added on a weight basis.

2.4. Testing of the filling ability property of the fresh HPSCC

Using an Abram's slump cone, the slump flow was performed to assess the fresh HPSCC concrete's filling ability [32]. Without applying any kind of compaction, the freshly mixed concrete was poured into the cone in a single layer. After the fresh concrete had been within the cone for approximately five (5) seconds, the cone was raised upright, allowing the fresh concrete to deform over the surface of the non-absorbing pan. The T_{500} slump flow time value was recorded by noting the amount of time it took for the freshly laid concrete to reach the 500 mm spread circle while also starting a stopwatch. At each of the four locations where the flow patty was divided into eight equal segments, the diameter of the concrete spread was measured. According to EFNARC [33], the average diameter was utilized to express the concrete's slump flow. This is seen in Fig. 4.

Fig. 4: Slump flow test.

2.5. Preparation of the hardened HPSCC

The specimens required for testing were prepared through several steps such as moulding, de-moulding and water-curing. Cube specimens of 150 mm (length) x 150 mm (breadth) x 150 mm (height) were used to conduct the compressive strength. Pouring of the fresh HPSCC inside the mould was done in just a single layer, with no form of compaction. Sealing of the samples were done with a non-absorbing material while it was well placed without being disturbed at room temperature. After 24±4 hours de-moulding, marking and transferring of the concrete samples into the curing tank were carried out for wet curing by water ponding. The wet curing by water ponding was done, till the days they were tested. The ASTM standard practice [31] was followed for curing. The curing temperature was $23\pm2\ ^{0}C$ and the relative humidity was above 95%.

2.6. Testing of the compressive strength property of the hardened HPSCC

In order to determine the compressive strength of the concrete, a compression test was performed. At the water-curing ages of 7, 28, and 56 days, the compression test was performed in accordance with ASTM standard [34]. Fig. 5 shows the compression device in use, a Model YES-2000 with a 2000 kN maximum capacity and a rate of loading of 140 kg/cm^2 per minute was applied. At each age, 150 x 150 x 150 mm cubes were examined in triplicate. Fifty-four (54) concrete cubes were tested for the compressive strength. The specimen's maximum or ultimate load was recorded when compression was applied. The average of the results from three specimens was used to calculate the compressive strength based on the ultimate load and the cross-sectional area of the cube.

Fig. 5: Compression test.

3 Statistical data analysis of the strength properties of the HPSCC

Analysis of variance (ANOVA) two-way and one-way techniques, with MS-Excel tool and Minitab 18 software, respectively, were used to statistically analyze the response data of the compressive strength, in order to examine the variation in the measured compressive strength of the high

performance self-compacting concretes as well as to determine the optimum mix (that is, the factors that gave the best response). Concrete types (in terms of the percentage levels of replacement of IFS) in Table 4 and curing ages were systematically selected as the factors, while the compressive strength of the concrete was the dependent variable (the response). This is relevant in the construction industry, as the statistical analysis of these factors in response to the compressive strength, will inform the industry about the statistical significance of these factors to the response. The level of each significant factor's statistical significance in the model was then determined by obtaining the p-value for each significant factor. The statistical significance of the factors to the measured response is indicated by the p-value. The statistical significance of the factors to a particular response is greater if the p-value is less than 0.05. The statistical significance of the factors to a particular measured response is also reduced when the p-value is larger than or equal to 0.05 [35]. The lesser the p-value, the more statistically significant the IFS percentage replacements as well as the curing ages are to the compressive strength measured. The optimum mix was determined by examining the p-values of each concrete type. The concrete with the least p-value was taken as the optimum mix. Meaning that it is more statistically significant to the measured compressive strength than the other concrete types. Also, the curing age at which that was obtained was also noted.

Minitab 18 software was used to obtain the main effect plot for the compressive strength of the various HPSCC mixtures containing IFS, in order to determine the best possible level of mix proportion for optimization. That is, to maximize the compressive strength.

Minitab 18 software was also used to obtain the 3D response surface plot to determine the relationship that exists between the factors (independent variables, which are the IFS content and the curing age) and the measured response (dependent variable, which is the compressive strength), according to a similar work done by Oyebisi et al [36], but on cashew nut shell ash-based conventional concrete.

4 Empirical modeling

The empirical modelling of the filling ability property and the compressive strength, which are the key properties of the high-performance self-compacting concrete are discussed in this section.

4.1 Empirical modeling of the filling-ability property of the HPSCC

Empirical modeling was performed on the filling-ability characteristics of the fresh HPSCC, on the basis of the slump-flow and the volume of the paste of the fresh concrete. When slump flow test is carried out, deformation as a result of self –weight or gravity takes place, which does not stop until the point of equilibrium between the yield stress (τ_y) and the shear stress (S_f) is reached. At this point, the slump flow spread is measured [37]. The equilibrium between the yield stress and the slump flow, on the basis of research from previous study [38] is expressed in Equation (1).

$$\tau_y = \frac{\rho g V}{\frac{S_f}{2\pi(\frac{S_f}{2})^2}} = \alpha \frac{\rho}{{S_f}^2} \quad (1)$$

where:
g represents acceleration due to gravity, V represents the volume of the concrete in its fresh state, ρ represents the concrete density, S_f represents the fresh concrete slump flow and α represents a constant (2gV/π).

For any suspension that does not satisfy Newton's law, it is reported that the relationship between its yield stress and the volume of its solid contents can be expressed as in Equation (2) [39].

$$\tau_y = kS_v{}^3 \quad (2)$$

where:
S_v represents the volume of the solid contents, k is a constant of proportionality.

In the same vein, HPSCC is seen as a suspension, which contains fine aggregate and coarse aggregate that are suspended in the concrete paste and which does not also satisfy Newton's law. For this reason, Equation (2) can be modified into Equation (3) thus:

$$\tau_y = kS_v{}^n \quad (3)$$

S_v is as described before and n stands for a constant value. The water reducer and the void content of air formed part of the total volume of the paste (V_P). Therefore, considering a cubic meter (1 m^3) of the concrete, the volume of the solid content (S_v) was expressed in Equation (4) thus:

$$S_v = 1 - V_P \quad (4)$$

The above expression was used to generate a relationship between the volume of the binder paste and the slump-flow, as expressed in Equation (5).

$$\frac{\rho}{S_f{}^2} = \beta(1 - V_P)^n \quad (5)$$

where:
β also stands for a constant, based on the HPSCC slump-flow test data.

Equation (5) was expressed in Equation (6). further thus:

$$In\frac{\rho}{S_f{}^2} = In\{\beta(1 - V_P)^n\} = nIn(1 - V_P) + In\beta \quad (6)$$

V_p was derived from the volume ratios of the binders utilized in this research, the water reducer as well as the water used in this study. The logarithm values of $\rho/S_f{}^2$ as well as $(1-V_p)$ were plotted against each other, n and β were respectively the slope and the intercept of the plotted graph.

The relative density of the fresh HPSCC, ρ_r was used to replace the density, ρ above. Of which, $\rho_r = \rho/\rho_w$ and ρ_w represents the density of water at 24^0C, 1000 kg/m^3). Hence, Equation (7) was obtained:

$$\frac{\rho_r}{S_f{}^2} = 0.001\beta(1 - V_P)^n \quad (7)$$

4.2 Empirical model of the compressive strength

An empirical model was also generated for the compressive strength of the hardened HPSCC, that combined the parameters of the strength developed over time with the strength developed due to the addition of IFS. This is as presented in Equation (8).

$$f_c(t) = f(t, t_s)\ x\ f_{cs}(IFS) \quad (8)$$

where:
$f_c(t)$ represents the compressive strength generated at any time, t (in days), expressed in MPa, $f(t, t_s)$ represents the strength per time parameter, which is equal to 1, at 28 days compressive strength, expressed in MPa, while f_{cs} represents the compressive strength of the concrete, on the basis of IFS addition, expressed in MPa.

The 28 days' strength 'f_{c28}' is often utilized in specifying the concrete compressive strength. As a result of this, when f_{cs} was replaced with f_{c28}, Equation. (8) was modified to Equation (9):

$$f_c(t) = f(t, 28)\ x\ f_{C28}(IFS) \quad (9)$$

ACI [40] generated an expression for the strength per time parameter $f(t, 28)$, expressed in MPa, as seen in Equation (10):

$$f(t,28) = \frac{f_c(t)}{f_{C28}} = \frac{t}{\alpha+\beta t} \quad (10)$$

The constant terms are the α and the β, which are dependent on the curing ages, type of concrete as well as the type of cement used. These constants were obtained when *1/f(t, 28)* was plotted against 1/t, of which t represents the curing ages investigated in this research, which were 7 days, 28 days and 56 days.

In the presence of IFS, the compressive strength of the 28 days increased. With an increase in IFS content, the rise in strength varied polynomially. Equation (11) illustrates the polynomial relationship between IFS content and its contribution to compressive strength over 28 days.

$$f_{ccr28} = A(P_{ifs})^2 + BP_{ifs} + C \quad (11)$$

where:
P_{ifs} is the weight-based percentage of IFS in the total binder or cementing ingredients, expressed in %, and f_{ccr28} is the strength contribution of IFS toward the concrete's compressive strength at 28 days, expressed in MPa.

Lastly, the following expression for the compressive strength of concretes can be produced in Equation (12) by inserting Equation (10) and Equation (11) in Equation (8):

$$f_c(t) = \frac{t}{\alpha+\beta t}(A(P_{ifs})^2 + BP_{ifs} + C) \quad (12)$$

where:
$f_c(t)$ – Concrete's age-dependent compressive strength [MPa],
t^c – Concrete's age [days],
P_{ifs} – Concrete's percentage IFS content [%B].

5 Research results and analysis

The results obtained in this and their analyses are presented in this section.

5.1 Filling ability property of the fresh high performance self-compacting concrete

The results of the fresh HPSCC mixtures for slump flow and slump flow time (T_{500} time) by Abram's cone are presented in Table 5.

Table 5: Properties of the fresh HPSCC.

Concrete Type	Slump flow [mm]	T_{500} slump flow time [seconds]
HPSCC0,100.	687	2.59
HPSCC10,90	685	2.80
HPSCC20,80	680	3.72
HPSCC30,70	670	3.84
HPSCC40,60	657	3.93
HPSCC50,50	652	3.97
EFNARC Standard [33]	550 - 850	2 - 5

The results for the slump flow result ranged from 652 mm to 687 mm, demonstrating the strong HPSCC filling capabilities. The HPSCC slump flow typically ranges from 550 to 850 mm [33,41]. With more IFS content, the slump flow significantly decreased, as seen in Table 5. The increased paste volume and enhanced fineness of the IFS material are credited for this [3]. With a larger IFS component, the concrete paste volume increased. Because the collision between aggregates is substantially increased with a smaller inter-particle distance, the increased paste volume and the increased fineness of the binder demand more water to flow, which reduces the deformability of the concrete [4]. With some variations in the flow spread, the slump flow results showed the relative differences in the filling abilities of the concrete mixes. Consequently, it is advised to use the slump flow to evaluate the HPSCC's filling ability.

According to Table 5, the T_{500} slump flow times of the various HPSCC combinations ranged from 2.59 to 3.97 seconds. 2 to 5 seconds is the recommended range for T_{500} slump flow [33]. The various concrete types examined in this study had T_{500} slump flow times that were within the acceptable bounds. The T_{500} slump flow time value of the tested concrete increases as the IFS content does. It was recognized that there was more kinetic energy involved, which suggested that the concrete's plastic viscosity had increased [5]. A larger IFS content increased the binders' surface area and volume fraction. The viscosity of concretes often increases with an increase in volume fraction and surface area of binders, which in turn lengthens the time it takes for concrete to flow [42]. Likewise, the paste volume was increased with higher IFS content. The plastic viscosity of such concrete typically increases with an increase in concrete paste volume [43].

5.2 Compressive strength property of the hardened high performance self-compacting concrete

The results of the compressive strength property of the tested high performance self-compacting concrete types are presented in Fig. 6.

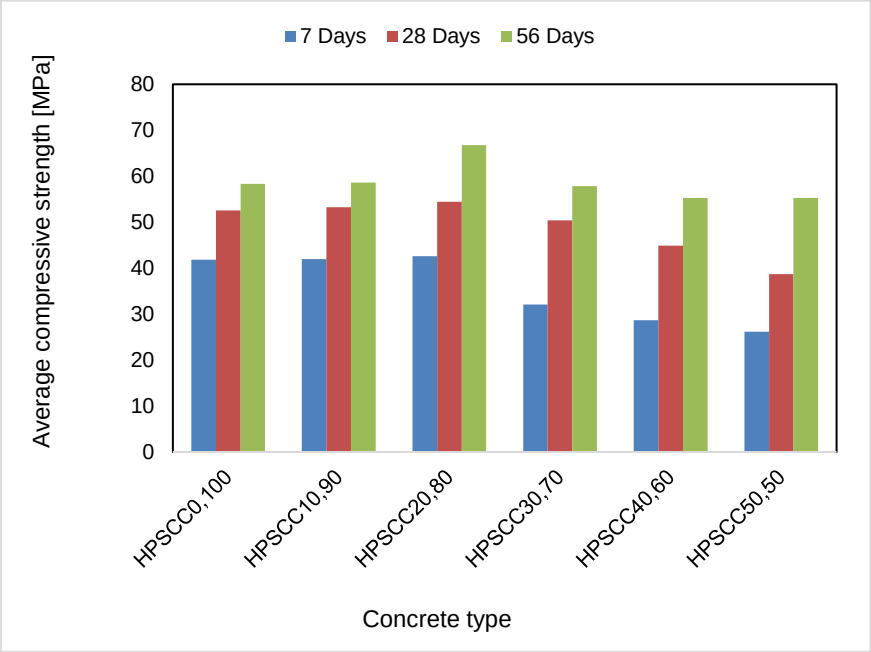

Fig. 6: Compressive strength of the tested HPSCC.

The compressive strength of the HPSCC increased, from the average compressive strength shown in Fig. 6, from 7 days to 56 days of curing as a result of cement hydration. The highest strength increments were achieved at the curing ages of 7 and 28 days. For the various types of concrete tested, the compressive strength at 28 days ranged from 38.67 to 54.44 MPa. Additionally, the concrete's compressive strength at 56 days ranged from 55.25 to 66.79 MPa. The HPSCC20,80, which contains 20% IFS and 80% OPC, had the highest amount of later-age compressive strength. On the other hand, HPSCC50,50, which was made using 50% IFS and 50% OPC, had the lowest compressive strength for all of the curing days. Nevertheless, all HPSCCs met the specifications for the early-age and later-age compressive strengths of high-performance concrete [44]. Due to the employment of high-range water reducers (HRWR), which produced dense concretes with few voids, good compressive strength was developed. Because the porosity of the HPSCC was decreased, the compressive strength increased [30]. According to this study, the HPSCC's porosity decreased at low water/binder ratios. Consequently, it can be inferred that this reduction enhanced the microstructure of the HPSCC at the bulk paste matrix (BPM) and the interfacial transition zone (ITZ). Additionally, since the amount of water was the same for all concretes, there was an increased binder volume as a result of the low water/binder ratio. It was concluded that the increase in binder volume caused the fine and coarse aggregates to be tightly packed, which raised the calcium-silicate-hydrate (CSH) and increased the compressive strength. At ages 7, 28, and 56 days, the IFS greatly improved the compressive strength of concretes. IFS's pozzolan composition and micro-filling characteristics, as well as the fact that it is a pozzolan, are mostly the reasons for the increase in compressive strength. The IFS can fill the concrete micro void with particles

of a smaller size. Similar to this, IFS chemically reacts with moisture and calcium hydroxide $Ca(OH)_2$, a by-product of cement hydration, to produce additional calcium silicate hydrate [45]. This additional calcium silicate hydrate acts as a crucial strength-contributing element and enhances the concrete's compressive strength. For the tested compressive strength, each type of the concrete met the performance requirements. However, using 10% and 20% IFS, the concrete's compressive strength was better. IFS content above 20%, however, made mixing and handling difficult because of too much cohesion or stickiness, especially at lower W/B ratios. As a result, 20% IFS content can be suggested as the ideal IFS content for the HPSCC that was tested.

5.3 Statistical analysis of the experimental data for the compressive strength

The statistical data analyses of the compressive strength of the tested HPSCCs are presented in Table 6 to Table 8 and Fig. 7.

Table 6: Factor information of the compressive strength of the tested HPSCCs.

Factor	Type	Levels	Values
IFS Content (%)	Fixed	6	0, 10, 20, 30, 40, 50
Curing Age (Days)	Fixed	3	7, 28, 56

Table 7: Analysis of variance of the compressive strength of the tested HPSCCs.

Source	DF	Adj. SS	Adj. MS	F-Value	P-Value
IFS Content (%)	5	459.72	91.943	9.76	0.001
Curing Age (days)	2	1618.88	809.438	85.88	0.000
Error	10	94.25	9.425		
Total	17	2172.84			

Table 8: Simple main effect analysis of the compressive strength of the tested HPSCCs.

Term	Coef	SE Coef	T-Value	P-Value	VIF
Constant	47.759	0.724	66.00	0.000	
IFS Content (%)					
0	3.18	1.62	1.96	0.078	1.67
10	3.51	1.62	2.17	0.055	1.67
20	6.85	1.62	4.23	0.002	1.67
30	-1.00	1.62	-0.62	0.552	1.67
40	-4.82	1.62	-2.98	0.014	1.67
Curing Age (Days)					
7	-12.20	1.02	-11.92	0.000	1.33
28	1.27	1.02	1.24	0.242	1.33

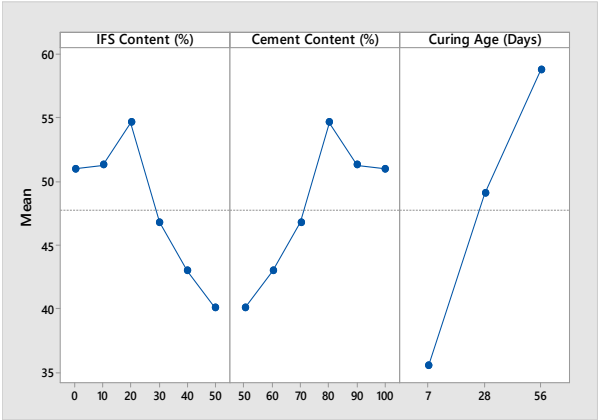

a)

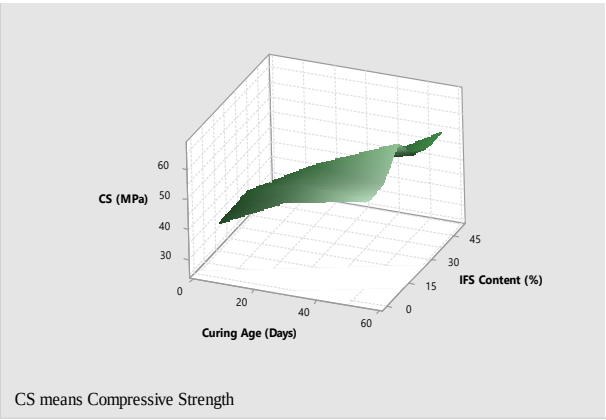

b)

Fig. 7: Statistical analyses of the compressive strength: a) Main effect plot for the compressive strength, b) 3D surface plot.

There was a statistically significant effect of the percentage replacement levels of induction furnace slag and the curing ages on the concrete compressive strength. This can be seen from the interaction effect analysis on Table 7. The p-values obtained for the IFS contribution and the curing age contribution were 0.001 and 0.000 respectively. These values were less than 0.05. This means that they are statistically significant to the measured response which is the compressive strength [46,47].

For the simple main effect analysis on Table 8, 20% IFS with p-value of 0.002, less than 0.005 has more statistical significance on the compressive strength, while 0% with p-value of 0.078, greater than 0.005 has the least statistical significance on the compressive strength. This justifies the report in section 5.2 that 20% IFS is the optimum mix for the tested HPSCCs. In the same vein 7 days curing age with p-value of 0.000, less than 0.05 has more statistically significant effect on the compressive strength than 28 days and 56 days. This also justifies the discussion in section 5.2 that greater strength development occurred between 7 and 28 days.

The main effect plot from Fig. 7a) revealed the peak compressive strength at 20% IFS, 80% cement and 56 days curing age. This also justifies that the best possible level of mix proportion for maximization of compressive strength is HPSCC20,80 at 56 days curing age [46,47].

The 3D surface plots from Fig. 7b) also showed that linear relationship exists between the compressive strength and the curing age, while polynomial relationship exists between the compressive strength and the IFS content. This justifies the empirical model equation generated in Eq. {2.12}.

6 Empirical models

The results of the empirical models and their discussions are presented in this section.

6.1 Empirical model of the filling ability of the HPSCC

Fig. 8 shows the correlation that exists between the HPSCC slump-flow (filling-ability) characteristics and the total volume of the fresh concrete paste, when induction furnace slag is partially replaced with 42.5 R Portland cement.

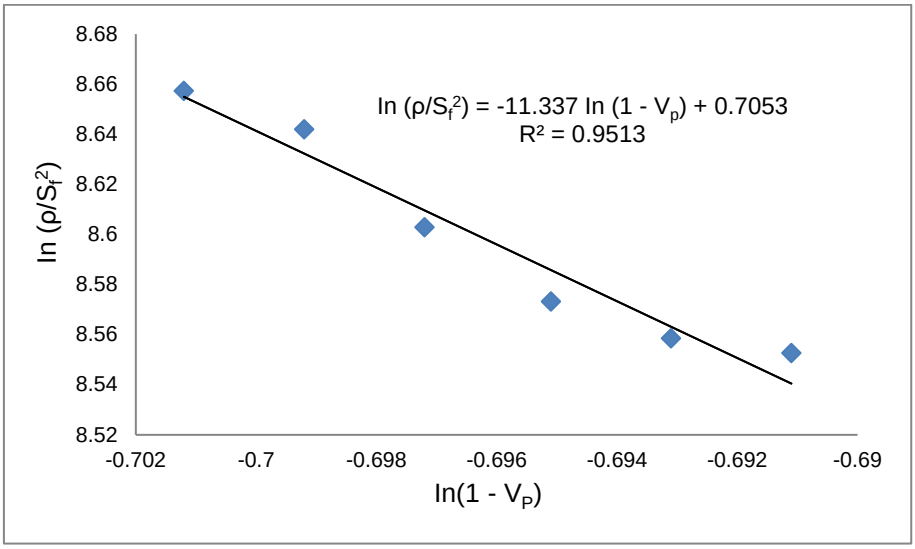

Fig. 8: Relationship between (ρ/S_f^2) and ($1-V_p$).

The relationship from Fig. 8, gave the empirical constants *n* (the slope of the plotted graph) and *β* (the intercept of the plotted graph) to be -11.337 and 2.0245, respectively. This makes Equation (7) to be re-written as in Equation (13):

$$\frac{\rho}{s_{f^2}} = 0.002(1 - V_P)^{-11.34} \quad (13)$$

The terms are as explained in section 4.1.

The correlation between the measured slump-flow (MSF) and the predicted slump-flow (PSF) of the various tested concrete is presented in Fig. 9.

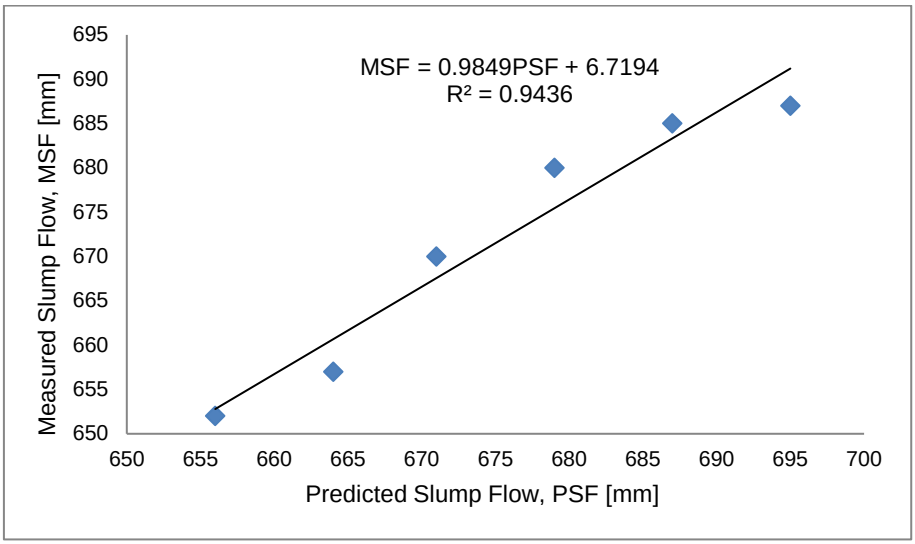

Fig. 9: Comparison between measured and predicted slump flows.

The empirical model for the filling-ability characteristics of the fresh HPSCC generated above in Equation (13), applies to the values of HPSCC volume of paste (V_P), ranging between 0.499 to 0.504 m^3/m^3. According to the ACI Committee [40], the volume of HPSCC paste usually falls within the range of 0.28 and 0.60 m^3/m^3. Also, this empirical model can be used for HPSCC, containing or not containing induction furnace slag. Likewise, this filling-ability model for HPSCC was derived for the values of slump-flow, ranging between 652 mm and 687 mm. According to SCCEPG [41], the values of the slump flow of HPSCC mostly falls within the range of 550 mm and 850 mm. Therefore, this model is valid for use in HPSCC, with the sump flow value falling within this standard range.

The major factors that influence the generality of this model include the type and the quantity of the superplasticizer utilized. It is also influenced by the level of how compatible, the binders and the superplasticizer are. A slump flow can be altered, without affecting the volume of the fresh HPSCC paste, by the influence of the quantity of the superplasticizer and also on the basis of the level of the compatibility between the binders and the superplasticizer [29].

From Fig. 9, showing the correlation between the measured slump-flow (MSF) and the predicted slump-flow (PSF), there was a strong and a linear relationship between the MSF and the PSF, with a coefficient of determination (R^2) of 0.944, resulting in a correlation coefficient of 0.972. This depicts that more than 95% of the slump-flow measured were accounted for, in the model generated.

When the slump-flow (S_f) of a particular fresh HPSCC is known, this generated model equation can be utilized to estimate the volume of paste (V_P) in such a concrete. As a result, helps fast-track the design of such an HPSCC mix, because, once the volume of the paste is established for a particular water-binder proportion, the quantity of the binder can be obtained. Likewise, for a specific quantity of binder, the quantity of the water to be used can be established. Lastly, with this filling-ability model for HPSCC containing IFS as an SCM, the passing ability of the HPSCC containing IFS as an SCM can be easily predicted because, filling-ability correlates strongly with passing-ability, as reported by Mark et al [5].

6.2 Empirical model of the compressive strength of the HPSCC

A strong and a linear correlation exist between the function relating to the 28 days' compressive strength [*1/f(t,28)*] and the function relating to the strength developed at the other curing ages, investigated in this research [*1/t*], as presented in Fig. 10. This depicts that the 28 days' compressive strength can be used to strongly predict the compressive strength, at any other age of curing. The empirical constants α and β obtained from Fig. 10 gave 4.52 and 0.78, respectively. These values fell within the range specified by ACI [40] that the values of α ranges between 0.05 and 9.25, while the

values of β ranges between 0.67 and 0.98. therefore, inserting the values of α and β into Equation (10), gives Equation (14):

$$f(t,28) = \frac{t}{4.52+0.78t} \quad (14)$$

From Fig. 11, a strong and a polynomial relationship exist between the 28 days' compressive strength and the percentage replacement variation of IFS with 42.5R Portland cement. This is expressed mathematically, as seen in Equation (15).

$$f_{ccr28} = -0.0109(P_{ifs})^2 + 0.2632P_{ifs} + 52.446 \quad (15)$$

where:
P_{ifs} represents the percentage replacement quantity of the induction furnace slag in each HPSCC tested, measured in weight. f_{ccr28} represents the equivalent 28 days' compressive strength of each percentage replacement of the IFS with 42.5R Portland cement.

It can also be seen from Fig. 11 that as the IFS content increased, the 28 days' compressive strength likewise increased up to 20%, before decreasing.

Lastly, inserting Equation (14) and Equation (15) in Equation (12), the generated empirical model for the compressive strength of the HPSCC, containing IFS as an SCM is expressed in Equation (16) thus:

$$f_c(t) = \frac{t}{4.52+0.78t}\,(-0.0109(P_{ifs})^2 + 0.2632P_{ifs} + 52.446) \quad (16)$$

where:
$f_c(t)$ represents the HPSCC compressive strength at a particular curing age, in MPa, t represents the curing age, in days and P_{ifs} represents the per cent IFS content of concrete (%B).

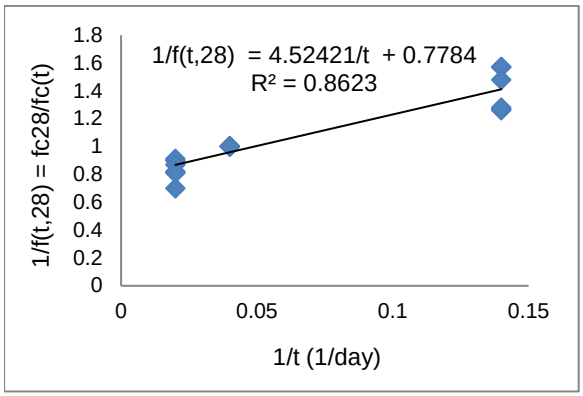

Fig. 10: Correlation of 1/f(t,28) with 1/t.

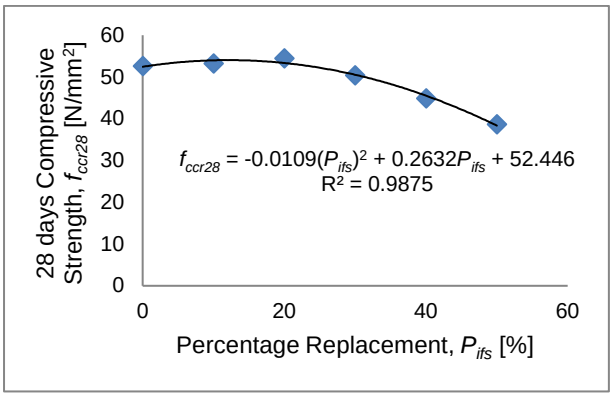

Fig. 11: Effect of IFS on the compressive strength of HPSCC at 28 days curing.

The relationship between the predicted compressive strength (PCS), using the generated empirical model Equation (16), at 28 days and the measured compressive strength (MCS), from the laboratory test, at 28 days, for all the HPSCC types tested in this study is presented in Fig. 12. Likewise, the correlation between the MCS and the PCS for all the concrete types tested, at all the curing ages investigated in this study is presented in Fig. 13.

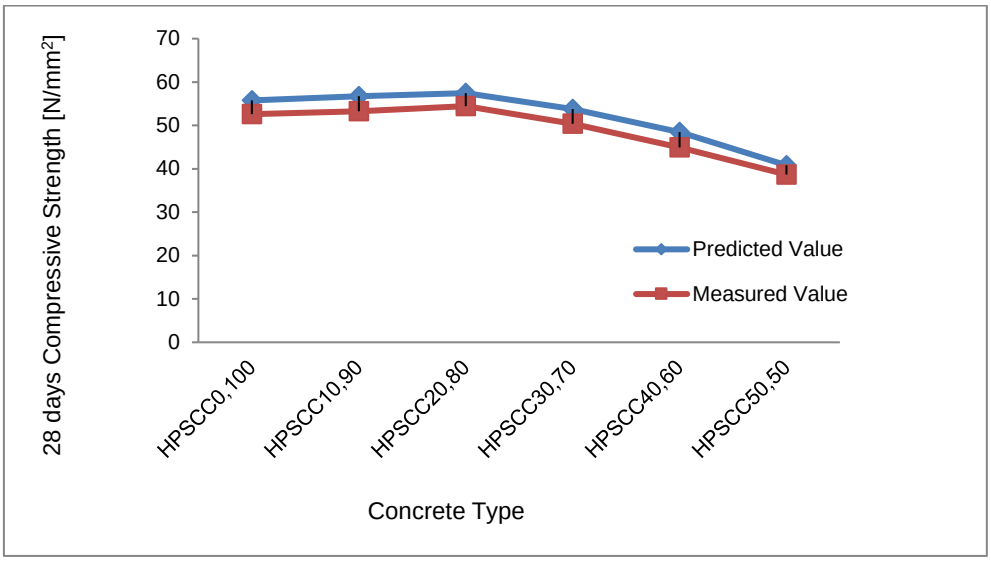

Fig. 12: Predicted and measured compressive strengths at 28 days.

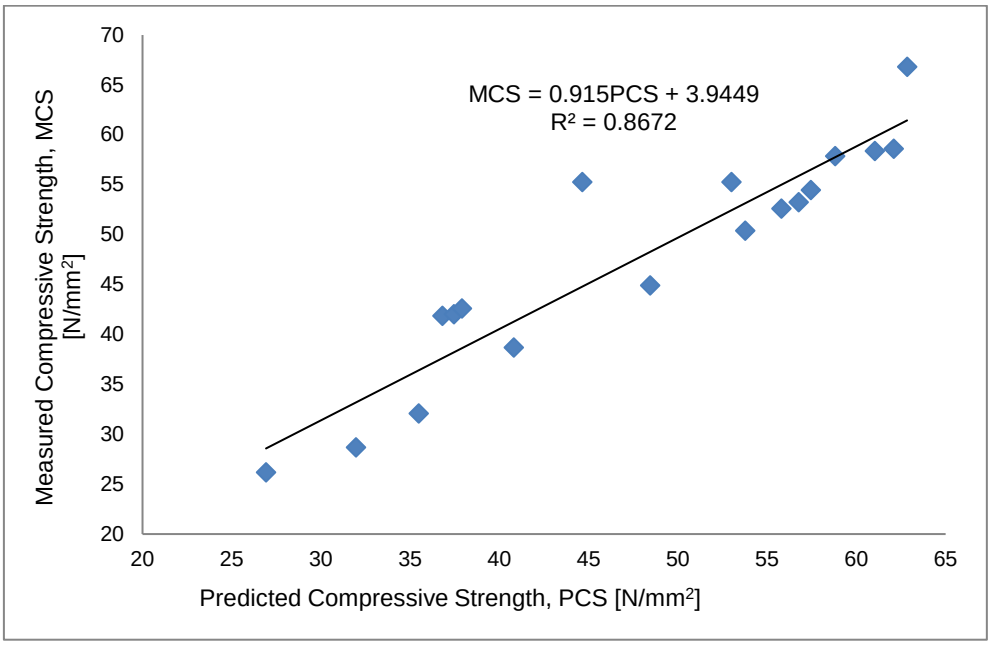

Fig. 13: Comparison between predicted and measured compressive strength of all the tested concrete types.

From Fig. 12, the 28 days' PCS and MCS correlated well. This was further confirmed from the excellent linear relationship between the measured and predicted compressive strength of all the concrete types and at all the curing ages investigated in this research, as seen in Fig. 13, having a coefficient of determination (R^2) of 0.8672 and an equivalent correlation coefficient (R) of 0.9312. This depicts that more than 86% of the compressive strength measured were accounted for, in the model generated. This compressive strength model (Equation 16) generated in this study, is applicable to an HPSCC mix of water-binder proportion, ranging between 0.30 and 0.50 and air entrained. It is also valid for HPSCC containing IFS as an SCM, at percentage replacement levels of 0% to 50% with 42.5R Portland cement (ASTM Type I cement) and cured in water only.

Available charts of strength can be easily used to estimate the compressive strength of the ordinary conventional concrete [15]. This is not so with HPSCC, because it contains supplementary cementitious materials, whereby, the strength estimate of such HPSCC is on the basis of the pozzolanicity of the SCM, the rate of dilution process, the rate of hydration of the cement and the micro-filling nature of the binders [13]. Thus, this compressive strength model can be utilized in evaluating the mean compressive strength of HPSCC, having IFS as an SCM, in design stages. Likewise, for any

targeted compressive strength, this model can be adopted in determining the percentage replacement level of 42.5R Portland cement with the IFS. This is important for engineers and concrete practitioners in the construction industry.

7 Conclusions

The conclusions drawn from this study are as follows:

1) The materials utilized in producing the HPSCC in this study were suitable enough, as they were within the standard ranges of the chemical and the physical properties specification.

2) The characteristics of the fresh HPSCC complied with the standard specifications.

3) The strength properties of the HPSCCs were improved with the addition of the IFS, due to its micro filling and pozzolanic effects.

4) The statistical analyses revealed that the IFS and the curing age have statistically significant effect on the HPSCC strength characteristics.

5) Based on this research, both the experimental and the statistical analyses gave an optimum mix proportion of 20% IFS and 80% OPC, which is the concrete type HPSCC20,80.

6) The empirical models of the HPSCC provided, predicted values close to the measured values of the filling-ability and the compressive strength of the HPSCC tested. More than 86% of the measured values were accounted for, in the two models generated in this study. Therefore, the empirical model equation for the filling-ability property of the HPSCC containing induction furnace slag is $\frac{\rho}{s_{f^2}} = 0.002(1 - V_P)^{-11.34}$, while that of its compressive strength is $f_c\ (t) = \frac{t}{4.52+0.78t}$ (-0.0109$(P_{ifs})^2$ + 0.2632P_{ifs} + 52.446).

The incorporation of IFS as an SCM, in making an HPSCC is achievable. This study has successfully contributed to the body of knowledge, in the sense that, it has successfully investigated the use of IFS in making a more eco-friendly HPSCC, thereby, reducing the harmful effects of cement production in HPSCC making and also reducing the disposal of this IFS as a waste, which could have caused adverse effects on the environment. This reaserch has also successfully generated empirical models for the design of HPSCC and prediction of its filling ability and compressive strength, using induction furnace slag as a supplementary cementitious material.

Declaration of Competing interest

The authors hereby declare no conflict of interest, as far as this article is concerned.

Data availability

The data used to support the findings of this study are included within the article.

Acknowledgements

The authors would like to appreciate the management of Covenant University and CUCRID for their support at all times.

Credit authorship contribution statement

Mark Oluwaseun: Conceptualization, Data curation, Investigation. **Ede Anthony:** Formal analysis, Visualization, **Arum Chinwuba:** Writing – review. **Jolayemi Kayode:** Editing.

References

[1] WEI-TING, L.- KINGA, K. - MAREK, H. - MICHAL, L.- JANUSZ, M.: Engineering Properties of Ternary Cementless Blended Materials, International Journal of Engineering and Technology Innovation, 2020, vol. 10, no. 3, pp. 191-199, DOI: 10.46604/ijeti.2020.5201.

[2] HASSAN, A. - KIBRIA, M. G. - HASSAN, F. M.: Effects of Incorporating Recycled Brick and Stone Aggregate as Replacement of Natural Stone Aggregate in Concrete, International Journal of Engineering and Technology Innovation, 2019, vol. 9, no. 1, pp. 38-48.

[3] MARK, O.- EDE, A. - ARUM, C. - OYEBISI, S. Effects of Induction-Furnace Slag on Strength Properties of Self-Compacting Concrete, Civil and Environmental Engineering, 2021, vol. 17, no. 2, pp 513-527, DOI: 10.2478/cee-2021-0053.

[4] MARK, O. - EDE, A. - ARUM, C. - JOLAYEMI, K. - OJUAWO, I. - AJIMALOFIN, D. - ADEDIRAN, J. - BABATUNDE, I. - OLIMARO, G.: Fresh Characteristics of High-Performance Self-Compacting Concrete Using Induction Furnace Slag as Supplementary Cementitious Material, in Proceedings of the IOP Conference Series: Materials Science and Engineering, **1036** 012042, IOP Publishing, 2021, pp. 1-15, **DOI:** 10.1088/1757-899X/1036/1/012042.
[5] MARK, O. - EDE, A. - ARUM, C. - AWOYERA, P.: Strength and Durability Assessments of Induction Furnace Slag-Quarry Dust-Based High Performance Self-Compacting Concrete, Civil and Environmental Engineering, 2022, vol. 18, no. 1, pp 1-16, DOI: https://doi.org/10.2478/cee-2022-0001.
[6] FARHAD, A. - GUOWEI, M. - DOMINIC, L. - GOJKO, M.: Development of High-Performance Self-Compacting Concrete Using Waste Recycled Concrete Aggregates and Rubber Granules, Journal of Cleaner Production, 2018, vol. 182, no. 1, pp. 553-566, DOI: 10.1016/j.jclepro.2018.02.074.
[7] MA, J. - DIETZ, J.: Ultra High Performance Self Compacting Concrete, LACER, 2019, vol. 12, no. 7, pp. 33-42, DOI: https://www.researchgate.net/publication/237771202.
[8] RUSHING, M. - OZBAY, E. - OZTAS, A. - YUCE, M.: Appraisal of Long Term Effect of Fly Ash and Silica Fume on Compressive Strength of Concrete by Neural Networks, Construction and Building Materials, 2018, vol.21, no. 2, pp. 384-394, DOI: 10.1016/j.conbuildmat.2005.08.009.
[9] MURATA, J.: Flow and Deformation of Fresh Concrete, Materials and Structures, 2014, vol. 17, no. 1, pp. 117-129, DOI: 10.1007/BF02473663.
[10] TANIGAWA, Y. - MORI, H.- KUROKAWA, Y. - KOMURA, R.: Rheological Study on Slumping Behaviour of Fresh Concrete, Journal of the Japan Concrete Institute, 2012, vol. 14, no. 4, pp. 1-8, DOI: 10.3130/AIJS.59.1_8.
[11] CHIDIAC, S. - MAADANI, O. - RAZAGPUR, A. - MAIVAGANAM, M.: Controlling the Quality of Fresh Concrete – A New Approach", Journal of Concrete Research, 2018, vol. 52, no. 3, pp. 353-363, DOI: 10.1680/macr.52.5.353.
[12] DUVAL, R. - KADRI, E.: Influence of Silica Fume on the Workability and the Compressive Strength of High Performance Concrete, Cement and Concrete Research, 2018, vol. 28, no. 7, pp. 533-547, DOI: https://doi.org/10.1016/S0008-8846(98)00010-6.
[13] DE LARRARD, F.: A mix performance method for high performance concrete. London, UK: CRC Press, 1992.
[14] GUTIERREZ, P. - CANOVAS, M.: High Performance Concrete: Requirements for Constituent Materials and Mix Proportioning, ACI Materials Journal, 2016, vol. 93, no. 10, pp. 233-241, DOI:10.14359/9807.
[15] VIDELA, A. - GAEDICKE, C.: Modeling Portland Blast-Furnace Slag Cement High Performance Concrete, ACI Materials Journal, 2014, vol. 101, no. 5, pp. 365-375, DOI:10.14359/13422.
[16] BUI, V. - MONTGOMERY, D. - HINCZAK, I. - TURNER, K.: Rapid Testing Method for Segregation Resistance of Self-Compacting Concrete, Cement and Concrete Research, 2018, vol. 32, no. 4, pp. 1489-1496, DOI: https://doi.org/10.1016/S0008-8846(02)00811-6.
[17] GHEZAL, A. - KHAYAT, K.: Optimizing Self-Consolidating Concrete with Limestone Filler by Using Statistical Factorial Design Methods, ACI Materials Journal, 2016, pp. 264-272, DOI:10.14359/11972.
[18] JOULAZADEH, M. H. - JOULAZADEH, F.: Slag, Value Added Steel Industry By Products, Archives of Metallurgy and Materials, 2016, vol. 55, pp. 1137-1145, DOI: 10.2478/v10172-010-0017-1.
[19] ANDREWS, A. - GIKUNOO, E. - OFOSU, M. - TOFAH, H.: Chemical and Mineralogical Characterization of Ghanaian Foundry Slags, Journal of Minerals and Materials Characterization and Engineering, 2017, vol.11, pp. 183-191, DOI: 10.4236/jmmce.2012.112015.
[20] ASTM C 150: Standard specification for Portland cement. West Conshohocken, USA, ASTM International 2020, DOI: 10.1520/C0150_C0150M-16.
[21] ASTM C 494: Standard specification for chemical admixtures for concrete. West Conshohocken, USA, ASTM International 2020, DOI: 10.1520/C0494_C0494M-17.
[22] ASTM C 989: Standard specification for slag cement for use in concrete and mortars. West Conshohocken, USA, ASTM International 2020, DOI: 10.1520/C0989-10.
[23] ASTM C 125: Standard terminology relating to concrete and concrete aggregates. West Conshohocken, USA, ASTM International 2020, DOI: 10.1520/C0125-21A.
[24] NEHDI, M. - CHABIB, H. - NAGGAR, H.: Cost Effective SCC for Deep Foundations, Concrete International Journal, 2019, vol. 25, no. 6, pp. 95-103.
[25] ASTM C 618: Standard specification for coal fly ash and raw or calcined natural pozzolan for use as a mineral admixture in concrete. West Conshohocken, USA, ASTM International 2020, DOI: 10.14359/51725994.

[26] ASTM C 70: Standard test method for surface moisture in aggregates. West Conshohocken, USA, ASTM International, 2020, DOI: 10.1520/C0070-20.
[27] KOSMATKA, S. - KERKHOFF, B. - Panarese, W. - MacGrath, R.: Design and control of concrete mixtures. Ontario, Canada: Cement Association of Canada, 2018.
[28] ASTM C 33: Standard specification for concrete aggregate. West Conshohocken, USA, ASTM International 2020, DOI: 10.1520/C0033.
[29] HU, J. - WANG, K.: Effects of Aggregates on Flow Properties of Mortar, in Proceedings of the mid-continent transportation research conference. Ame, Lowa: Lowa State University, 2005, pp. 1-8.
[30] NEVILLE, A.: Properties of concrete. New York, USA: John Wiley & Sons, Inc., 2016.
[31] ASTM C 192: Standard practice for making and curing concrete test specimens in thw laboratory. West Conshohocken, USA, ASTM International 2020, DOI: 10.1520_C0192M.
[32] ASTM C 143: Standard test method for slump of hydraulic cement concrete. West Conshohocken, USA, ASTM International 2020, DOI: 10.1520/C0143_C0143M.
[33] EFNARC: Specifications and guidelines for self-compacting concrete. 2002.
[34] ASTM C 39: Standard test method for compressive strength of concrete specimens. West Conshohocken, USA, ASTM International 2020, DOI: 10.1520/C0039_C0039M.
[35] HINKELMANN, K. - KEMPTHORNE, O.: Design and analysis of experiment. London, UK: John Wiley & Sons, Inc., 2018.
[36] OYEBISI, S. - OWAMAH, H. - ALOMAYRI, T. - EDE, A.: Modeling the Strength of Cashew Nutshell Ash-Cement-Based Concrete, Magazine of Concrete Research, 2022, vol. 74, no. 10, pp. 487-496, DOI:10.1680/jmacr.20.00349.
[37] SUGITA, S. - YU, Q. - SHOYA, M. - TSUKINAGA, Y. - ISOJIMA, Y.: The Resistance of Rice Husk Ash Concrete to Carbonation, Acid Attack and Chloride Ion Penetration, in Proceedings of the Third CANMET/ACI International Conference on High Performance Concrete: Design and Materials and Recent Advances in Concrete Technology, 2017, vol. 11, pp. 29-43, DOI:10.14359/6124.
[38] MURATA, J.: Flow and Deformation of Fresh Concrete, Materials and Structures, 2014, vol. 17, pp. 117-129, DOI: 10.1007/BF02473663.
[39] TOMAS, D. G.: Transport Characteristics of Suspensions: Laminar Flow Properties of Flocculated Suspensions, Journal of American Institute for Chemical Engineers, 2016, vol. 7, pp. 431-437.
[40] ACI 209R: "Prediction of creep, shrinkage and temperature effects in concrete structures. Farmington Hills, USA, American Concrete Institute, 2020.
[41] SCCEPG: The European guideline for self-compacting concrete. Dublin, USA, International Bureau for Precast Concrete (BIBM), 2005.
[42] KIM, H. - PARK, Y. - NOH, J. - SONG, Y. - HAN, C. - KANG, S.: Rheological Properties of Self-Compacting High Performance Concrete, Proceedings of the CANMET/ACI International Conference. Michigan: ACI Publishers, 2017, pp. 653-668.
[43] STRUBLE, L. - HAWKINS, P.: Hydraulic cement. Philadelphia: ASTM STP 169 C, 2016, DOI: 10.1520/STP364395.
[44] Kaplan, M.: Compressive Strength and Ultrasonic Pulse Velocity Relationships for Concrete in Columns, ACI Journal, 2018, vol. 54, no. 6, pp. 675-688, DOI:10.14359/11462.
[45] YU, Q. - SAWAYAM, K. - SUGITA, S. - SHOYA, M. - ISOJIMA, Y.: The Reaction Between Rice Husk Ash and $Ca(OH)_2$ Solution and the Nature of its Product, Cement and Concrete Research, 2009, vol. 29, no. 4, pp. 37-43, DOI:10.1016/S0008-8846.
[46] Erdogan, A.: Determination of Optimum Conditions for Tyre Rubber in Asphalt Concrete, Building Environment Journal, 2019, vol. 40, no. 5, pp. 1492-1504, DOI:10.1016/j.buildenv.11.013.
[47] EDE, A. - GIDEON, A. - AKPABOT, A. - OYEBISI, S. - OLOFINNADE, O. - NDUKKA, D.: Review of the Properties of Lightweight Aggregate Concrete Produced from Recycled Plastic Waste sand Periwinkle Shells, Key Engineering Materials Journal, 2021, vol. 876, no. 3, pp. 83-87, DOI: 10.4028/KEM.876.83.